Archives of Mechanics • Archiwum Mechaniki Stosowanej • 30, 4–5, pp. 489–500, Warszawa 1978

An improved analysis of breakdown of thin liquid films

J. MIKIELEWICZ (GDAŃSK) and J. R. MOSZYŃSKI (DELAWARE)

IN EARLIER papers a simplified model of breakdown of thin liquid films was developed on the basis of some very strong physical assumptions concerning the nature of the film prior to breakdown and the velocity distribution in the rivulets which result from the breakdown. In the present paper the effect of relaxing these assumptions is investigated and it is found that for contact angles below about 60° the simplified analysis appears to be adequate, particularly in the light of uncertainties introduced by the condition of the surface.

We wcześniejszych pracach wykorzystywano model rozrywania cienkich warstw cieczowych na bazie kilku bardzo silnych założeń fizykalnych dotyczących natury warstw przed rozerwaniem i rozkładu prędkości w strugach powstałych wskutek rozerwania. W niniejszej pracy zbadano efekt złagodzenia tych założeń i wykazano, że dla kątów poniżej około 60° uproszczona analiza jest wystarczająca, w szczególności w świetle niepewności wprowadzonych przez strukturę i stan powierzchni.

В более ранних работах использована модель разрушения тонких жидкостных пленок на основе нескольких очень сильных физических предположений, касающихся природы пленок перед выступлением разрушения и распределения скоростей в потоках, возникающих вследствие разрушения. В настоящей работе исследован эффект смягчения этих предположений и показано, что для углов ниже примерно 60° упрощенный анализ является адекватным, в частности в свете неопределенностей введенных через условие поверхности.

Nomenclature

a, b, A, B, C, coefficients defined by Eqs. (3.10),
e_{rlv} energy of rivulets per unit width,
f function defined by Eq. $(2.8)_2$,
G_1 function defined by Eq. $(2.7)_2$,
G_2 function defined by Eq. $(2.11)_2$,
g gravitational acceleration,
h film thickness,
h_g^+ dimensionless film thickness defined by Eq. $(2.11)_1$,
h_s^+ dimensionless film thickness defined by Eq. $(2.7)_1$,
P_l pressure in the liquid phase,
P_v pressure in the vapor phase,
R radius of rivulet,
u velocity,
X ratio of wetted to total surface in rivulet regime [cf. Eq. (2.4′)]
x coordinate parallel to surface,
y coordinate normal to surface,
z complex variable,
ζ complex variable $(= \xi + i\eta)$,
θ contact angle,

http://rcin.org.pl

λ rivulet spacing,
μ viscosity,
ν kinematic viscosity,
ϱ density,
σ_{fg} surface tension between liquid and vapor,
σ_{sf} surface tension between solid and liquid,
τ shear stress,
ϕ function defined by Eq. $(2.8)_1$,
ψ integration variable,
Ψ function defined by Eq. (2.12).

1. Introduction

IN EARLIER papers [1, 2] the authors developed a theoretical model for the breakdown of thin liquid films driven, respectively, by shear at the free surface or by gravity. The model is based in part on the work of BANKOFF [3] and HOBLER [4, 5]. It assumes that an initially smooth laminar film flows isothermally down a vertical surface. Under certain conditions the film ruptures forming a series of rivulets whose cross-sections under the

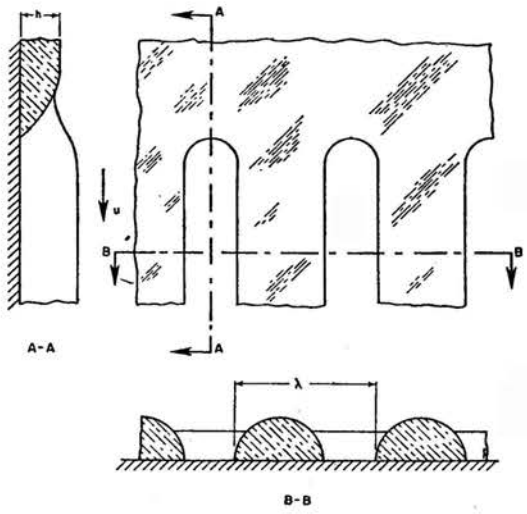

FIG. 1. Schematic of film breakdown.

assumption of the model are circular segments, as shown in Fig. 1. It is considered that for the rivulet configuration to remain stable three conditions must be satisfied:

1. The mass flow in the original film and in the rivulet configuration must be the same.

2. The total energy of the original film and of the rivulet configuration must be the same.

3. The total energy of the rivulet configuration must exhibit a local minimum.

Here, by "total energy" we mean the sum of the kinetic energy and the surface energy of all interfaces in the system.

http://rcin.org.pl

A further assumption made in references [1, 2] is that in the rivulets the velocity distribution at any transverse location x is the same as would occur in a uniform film of thickness $h(x)$ corresponding to the rivulet depth at that point.

While the experimental data available in the literature are hardly adequate to allow a full test of the model, the limited comparisons possible seem to be encouraging. This is particularly so if one considers the implications of some of the assumptions made. It is the purpose of the present paper to investigate the effect of relaxing some of the most drastic assumptions, particularly those concerning the smoothness of the film and the velocity distribution.

2. Summary of simplified model

Only the most important features and results of the analysis of references [1, 2] will be given here for ease of reference.

Under the assumption of constant temperature and vertical flow, the equation for the pressure difference between the liquid in the rivulets and the surrounding vapor

$$P_l - P_v = \frac{2\sigma}{R} \tag{2.1}$$

leads to $R = \text{const}$.

The three conditions listed in the Introduction may be formulated as follows:

$$\int_0^h \varrho u(y)\,dy = \frac{2}{\lambda}\int_0^{R\sin\theta}\int_0^{h(x)} \varrho u(x,y)\,dx\,dy; \tag{2.2}$$

$$\int_0^h \frac{\varrho}{2} u^2(y)\,dy + \sigma_{sf} + \sigma_{fg} = e_{\mathrm{riv}} = \frac{\varrho}{\lambda}\int_0^{R\sin\theta}\int_0^{h(x)} u^2(x,y)\,dx\,dy + \left[\frac{2R\theta}{\lambda} + \cos\theta - \frac{R\sin 2\theta}{\lambda}\right]\sigma_{fg} + \sigma_{fs}; \tag{2.3}$$

$$\frac{\partial e_{\mathrm{riv}}}{\partial X} = 0, \qquad \frac{\partial^2 e_{\mathrm{riv}}}{\partial X^2} > 0, \tag{2.4}$$

where

$$X = \frac{2R\sin\theta}{\lambda}. \tag{2.4'}$$

The three parameters of interest: the film thickness at breakdown h, the radius of resulting rivulets R and their spacing λ can be determined from Eqs. (2.2), (2.3) and (2.4). In practice the equations are recast yielding in the case of shear driven flow with the velocity distribution

$$u(y) = \frac{\tau}{\mu} y \tag{2.5}$$

http://rcin.org.pl

the following equation for the dimensionless film thickness h_s^+:

$$h_s^{+3}+(1-\cos\theta)-G_1(\theta)h_s^{+2}=0, \tag{2.6}$$

where

$$h_s^+ \equiv \left[\frac{\varrho\tau^2}{6\mu^2\sigma_{fg}}\right]^{1/3} h,$$

$$G_1(\theta) \equiv 3\cdot 2^{-2/3}\left[\frac{f(\theta)}{\sin\theta}\right]^{2/3}\frac{\sin\theta}{\phi(\theta)}\left[\frac{\theta}{\sin\theta}-\cos\theta\right]^{1/3}, \tag{2.7}$$

and

$$\phi(\theta)=\int_0^\theta(\cos\psi-\cos\theta)^2\cos\psi\,d\psi,$$

$$f(\theta)=\int_0^\theta(\cos\psi-\cos\theta)^3\cos\psi\,d\psi. \tag{2.8}$$

In the case of gravity driven flow the velocity distribution is

$$u(y)=\frac{g\varrho}{\mu}\left[\frac{y^2}{2}-yh\right] \tag{2.9}$$

and the equation for the dimensionless film thickness h_g^+ becomes

$$h_g^{+5}+(1-\cos\theta)-G_2(\theta)h_g^{+3}=0 \tag{2.10}$$

with

$$h_g^+ \equiv \left[\frac{\varrho^3 g^2}{15\mu^2\sigma_{fg}}\right]^{1/5} h,$$

$$G_2(\theta)=\frac{5}{2}\cdot\left[\frac{2}{3}\right]^{3/5}\frac{\sin\theta}{f(\theta)}\left[\frac{\Psi(\theta)}{\sin\theta}\right]^{3/5}\left[\frac{\theta}{\sin\theta}-\cos\theta\right]^{2/5}, \tag{2.11}$$

and

$$\Psi(\theta)=\int_0^\theta(\cos\psi-\cos\theta)^5\cos\psi\,d\psi. \tag{2.12}$$

In Eqs. (2.6) and (2.10) the leading terms represent the kinetic energy of the smooth, continuous films. The last term in each equation accounts for the kinetic and part of the surface energy of the rivulet systems, while the middle terms account for the remainder of the surface energy of the rivulet system and for the whole surface energy of the films.

It should be noted that for contact angles θ in the range from 0 to 90° both Eqs. (2.6) and (2.10) yield only one physically significant root, the others are either negative or imaginary or imply $X > 1$.

Among the most drastic assumptions stated above are those concerning the velocity distribution in the rivulets and the smoothness of the films. Their effect will be investigated below.

http://rcin.org.pl

3. Effect of improved velocity distribution in the rivulets

3.1. Shear driven flow

The velocity, $u(x, y)$, normal to the rivulet cross-sections shown in Fig. 2a is governed by the equation

$$\nabla^2 u = 0 \tag{3.1}$$

with the boundary conditions

$$u = 0 \quad \text{at} \quad y = 0, \tag{3.2}$$

$$\mu \frac{\partial u}{\partial n} = -\tau$$

on the outer surface ABC.

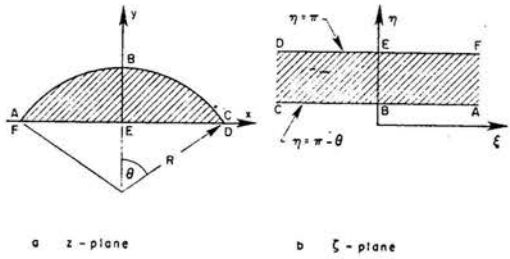

FIG. 2. Rivulet cross-section in the physical and transformed planes.

We assume for simplicity that $R\sin\theta = 1$, so that on ABC

$$x^2+y^2+2y\cot\theta = 1. \tag{3.3}$$

The problem is solved by mapping the physical z-plane conformally into the η-plane, shown in Fig. 2b, with the aid of the function

$$\zeta = \ln\frac{z-1}{z+1} \tag{3.4}$$

so that

$$\xi = \ln\left\{\frac{2y}{[(x+1)^2-y^2]\sin\eta}\right\}, \quad \eta = \tan^{-1}\frac{2y}{y^2+x^2-1}. \tag{3.5}$$

In the ζ—plane the transformed problem to be solved is

$$\frac{\partial^2 u}{\partial\zeta\partial\bar{\zeta}} = 0 \tag{3.6}$$

with the boundary conditions

$$u = 0 \quad \text{at} \quad \zeta = \zeta_1 = \xi+i\pi, \quad \bar{\zeta} = \bar{\zeta}_1 = \xi-i\pi,$$

$$\frac{\partial u}{\partial\zeta} - \frac{\partial u}{\partial\bar{\zeta}} = -\frac{\tau}{2\mu i}\frac{1}{\sinh\frac{\zeta}{2}\sinh\frac{\bar{\zeta}}{2}} \tag{3.7}$$

http://rcin.org.pl

at

$$\zeta = \zeta_2 = \xi + i(\pi - \theta), \quad \bar{\zeta} = \bar{\zeta}_2 = \xi - i(\pi - \theta).$$

The solution of the problems formulated in Eqs. (3.6) and (3.7) may be written

$$u = \frac{\tau}{2i\mu}\left[\frac{1}{\sinh\frac{\bar{\zeta}_1}{2}}\ln\left(\frac{\coth\frac{\zeta}{4}}{\coth\frac{\zeta_2}{4}}\right) - \frac{1}{\sinh\frac{\zeta_1}{2}}\ln\left(\frac{\coth\frac{\bar{\zeta}}{4}}{\coth\frac{\bar{\zeta}_2}{4}}\right)\right] \tag{3.8}$$

or

$$\frac{\mu u}{\tau} = \frac{1}{2}\left[a\ln\frac{A^2+B^2}{A^2+C^2} + 2b\left[\tan^{-1}\frac{B}{A} - \tan^{-1}\frac{C}{A}\right]\right], \tag{3.9}$$

where

$$a = \frac{\cosh\frac{\xi}{2}\cos\frac{\theta}{2}}{\sinh^2\frac{\xi}{2} + \cos^2\frac{\theta}{2}},$$

$$b = \frac{\sinh\frac{\xi}{2}\sin\frac{\theta}{2}}{\sinh^2\frac{\xi}{2} + \cos^2\frac{\theta}{2}}, \tag{3.10}$$

$$A = \sinh\frac{\xi}{2}\cos\frac{\pi+\eta}{4},$$

$$B = \cosh\frac{\xi}{2}\sin\frac{\pi+\eta}{4} + \sin\frac{\pi-\eta}{4},$$

$$C = \cosh\frac{\xi}{2}\sin\frac{\pi+\eta}{4} - \sin\frac{\pi-\eta}{4}.$$

In particular, on the centerline of the cross-section of the rivulet $\xi = 0$ and thus

$$\left(\frac{\mu u}{\tau}\right)_{\xi=0} = \frac{\ln\left(\tan\frac{\eta}{4}\right)}{\cos\frac{\theta}{2}}. \tag{3.11}$$

For contact angles of 30°, 60° and 90° Table 1 shows a comparison of the centerline velocity calculated from Eq. (3.11) with the straight line profile in a film. In attempting to compare the approximate calculations of mass flow and kinetic energy of references [1, 2] with the present results, we have calculated these quantities under the assumption that in each case $R\sin\theta = .1$. A comparison of the approximate and present, more exact, mass flow calculation is shown in Fig. 3 and that of kinetic energy in Fig. 4. It may be concluded that the error in kinetic energy for contact angles of less that 60° does not exceed 20%.

http://rcin.org.pl

Table 1.

	$\theta = 30°$		$y_{max} = 0.2679$			
$\frac{\mu u}{\tau} = y$	0.05	0.1	0.2	0.2679		
η	3.0417	2.9423	2.7468	2.6181		
$\frac{\mu u(0, \eta)}{\tau}$	0.0517	0.1033	0.2057	0.2741		
	$\theta = 60°$		$y_{max} = 0.5774$			
$\frac{\mu u}{\tau} = y$	0.1	0.2	0.2679	0.5774		
η	2.9423	2.7468	2.6181	2.1089		
$\frac{\mu u(0, \eta)}{\tau}$	0.1152	0.2294	0.3058	0.6246		
	$\theta = 90°$		$y_{max} = 1$			
$\frac{\mu u}{\tau} = y$	0.1	0.2	0.2679	0.5774	0.8	1
η	2.9423	2.7468	2.6181	2.1089	1.7921	1.5708
$\frac{\mu u(0, \eta)}{\tau}$	0.1412	0.2810	0.3745	0.7650	1.0362	1.2464

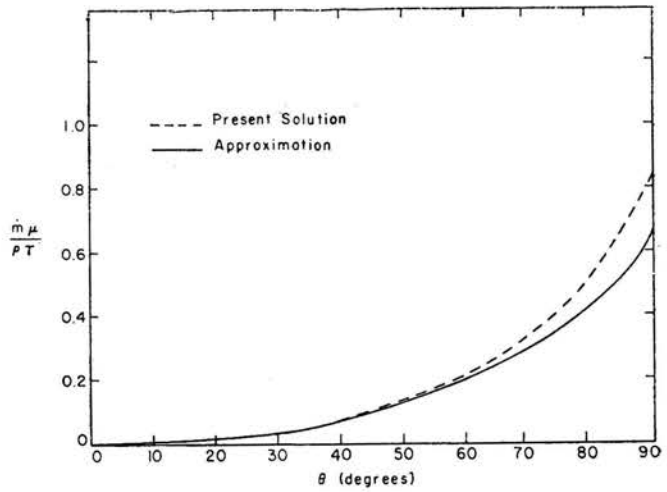

FIG. 3. Shear driven flow. Mass flow.

http://rcin.org.pl

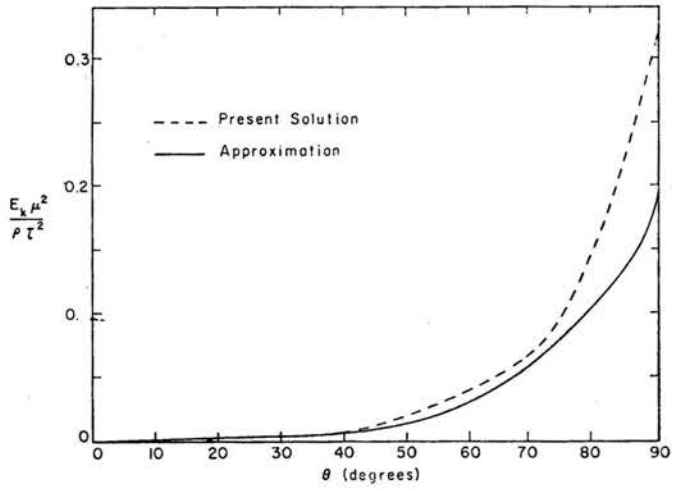

FIG. 4. Shear driven flow. Kinetic energy.

3.2. Gravity driven flow

With a falling film on a vertical surface Eqs. (3.1) and (3.2) are replaced by

$$\nabla^2 u + \frac{g}{\nu} = 0 \tag{3.12}$$

with the boundary conditions

$$u = 0 \quad \text{at} \quad y = 0, \tag{3.13}$$

$$\frac{\partial u}{\partial n} = 0$$

on the outer surface ABC.

Using the same mapping function, as in the previous case, Eqs. (3.12) and (3.13) transform into

$$2\frac{\partial^2 u}{\partial \zeta \partial \bar{\zeta}} + \frac{g}{\nu}\frac{1}{(\cosh\zeta - 1)(\cosh\bar{\zeta} - 1)} = 0 \tag{3.14}$$

and

$$u = 0 \quad \text{at} \quad \zeta = \zeta_1 = \xi + i\pi, \quad \bar{\zeta} = \bar{\zeta}_1 = \xi - i\pi,$$

$$\frac{\partial u}{\partial \eta} = \frac{\partial u}{\partial \zeta} - \frac{\partial u}{\partial \bar{\zeta}} = 0 \quad \text{at} \quad \zeta = \zeta_2 = \xi + i(\pi - \theta), \quad \bar{\zeta} = \bar{\zeta}_2 = \xi - i(\pi - \theta). \tag{3.15}$$

The solution of the above problem may be written

$$u = \frac{g}{2\nu}\left[-f(\zeta)f(\bar{\zeta}) + f(\bar{\zeta}_2)f(\zeta) + f(\zeta_2)f(\bar{\zeta}) + f(\zeta_1)f(\bar{\zeta}_1) - f(\bar{\zeta}_2)f(\zeta_1) - f(\bar{\zeta})f(\zeta_2)\right], \tag{3.16}$$

where

$$f(\zeta) = \frac{\cosh\zeta + 1}{\sinh\zeta} = \coth\frac{\zeta}{2} \tag{3.17}$$

http://rcin.org.pl

or

$$\frac{uv}{g} = \left[\frac{1}{2}\frac{\cosh\xi-1}{\cosh\xi+1} - \frac{1}{2}\frac{\cosh\xi+\cos\eta}{\cosh\xi-\cos\eta} - \frac{\sinh^2\xi}{\sinh^2\xi+(\cos\theta+1)(\cosh\xi+1)} + \frac{\sinh^2\xi+\sin\eta\sin\theta}{\sinh^2\xi+4\cos^2\frac{\eta}{2}\sin^2\frac{\theta}{2}-(\cos\eta-\cos\theta)(\cosh\xi+1)}\right]. \tag{3.18}$$

The centerline velocity distribution is given by

$$\frac{v}{g}u_{\xi=0} = -\frac{1}{2}\left(\frac{1+\cos\eta}{1-\cos\eta} - \frac{\sin\eta\sin\theta}{2\cos^2\frac{\eta}{2}\sin^2\frac{\theta}{2}-\cos\eta+\cos\theta}\right). \tag{3.19}$$

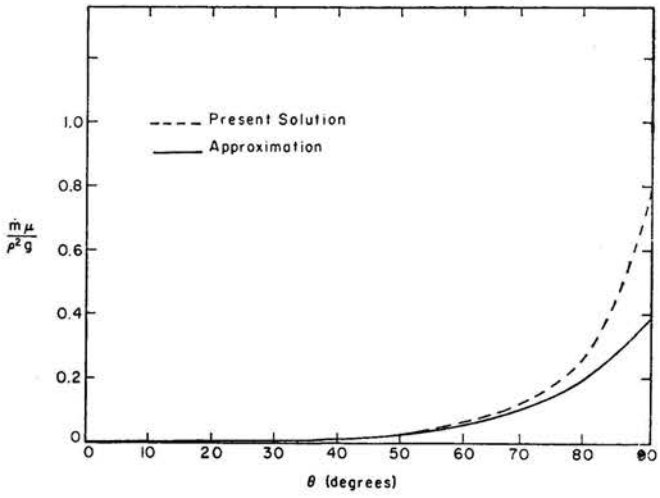

FIG. 5. Gravity driven flow. Mass flow.

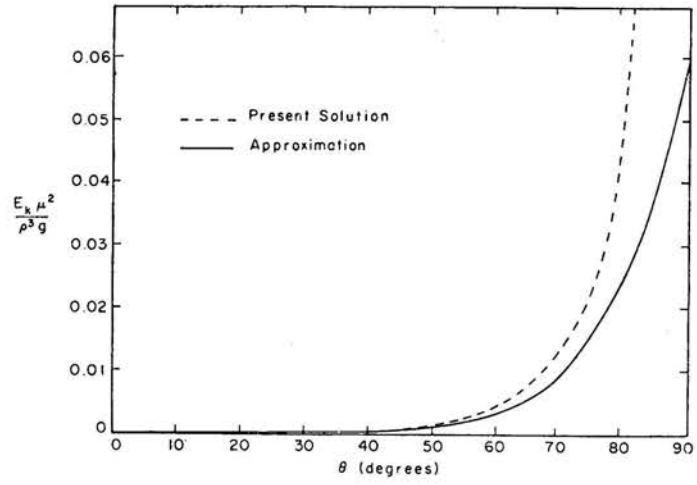

FIG. 6. Gravity driven flow. Kinetic energy.

http://rcin.org.pl

After some algebraic transformations it may be shown that the centerline velocity given by Eq. (3.19) is identical with the parabolic velocity distribution assumed for the film for all contact angles.

Figures 5 and 6 compare the mass flow and kinetic energy calculated respectively with the aid of the simplifying assumptions of references [1, 2] and from the present, more exact theory. It may be noted that while for contact angles below about 60°, the errors are quite small; they increase very rapidly for contact angles approaching 90 degrees. Although the actual values of the contact angles, to be used in applications of most immediate interest to the present authors, are still somewhat uncertain [6, 7], it would appear that for rivulets of water on "clean" metallic surfaces these angles are not likely to exceed 60°, rendering the earlier approximations acceptable.

4. Effect of film waviness

One of the most severe assumptions in the simple model of film breakdown is that the film is smooth and laminar. This is contrary to almost all available evidence, cf. for example references [8—10](1), which indicates that more or less complex wave patterns persist on thin films even at very low velocities and film thicknesses. The waves may be transverse, horseshoe-shaped and even longitudinal, as observed by several investigators. Any attempt to take these, often almost random, wave patterns into account in the theory would present a formidable undertaking. An alternative, although admittedly less satisfying approach, would be to investigate the effect of changes in the various computed quantities, which we might expect to be due to the film waviness, on the ultimate predictions of the model. This is the path adopted here, if only to provide a feeling for the magnitudes of effects to be expected.

As has been mentioned earlier the leading term in Eqs. (2.6) and (2.10) accounts for the kinetic energy of the film. It is assumed that the waviness of the film may be responsible for the kinetic energy being actually somewhat larger than that computed for a smooth film of a given mass flow. This term was thus multiplied by a factor $(1+\alpha)$ with α in the range from 0 to 0.4.

The second term in Eqs. (2.6) and (2.10) accounts for the difference between the surface energy of the film and the rivulets. A waviness of the film would lead to an increase in the surface energy of the film and thus to a modification of the second term from $(1-\cos\theta)$ to $(1+\beta-\cos\theta)$ with β ranging from 0 to 0.3.

Finally, very laborious calculations would be necessary to account for the more exact velocity profiles calculated in the preceding section for the rivulets. Instead, the effects of resulting increases in the kinetic energy of the rivulets could be investigated by allowing α and β to take on negative values.

The results of these calculations are shown for contact angles of 30° and 60° in Figs. 7 and 8. It should be noted that for some contact angles the full range of variation of α and β led to the disappearance of physically meaningful values of the minimum film thickness.

(1) This listing of experimental investigations of thin liquid films is only a small sample of a very rich literature. More extensive bibliographies are given in the references cited.

http://rcin.org.pl

In general it may be stated that errors in the calculation of kinetic energy of the film appear to have a weaker effect on the values of h^+ than errors in surface energy. The latter, in addition, are more important at low rather than at high values of the contact angle.

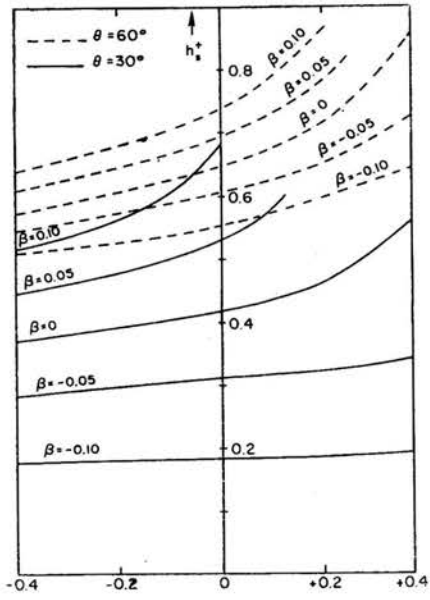

FIG. 7. Shear driven flow. Effect of errors due to film waviness on minimum film thickness.

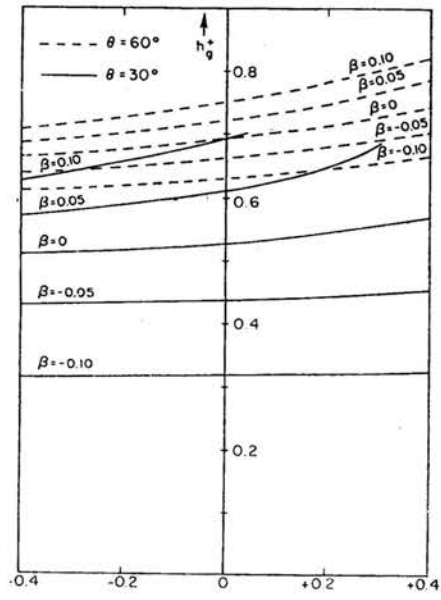

FIG. 8. Gravity driven flow. Effect of errors due to film waviness on minimum film thickness.

5. Conclusions

The calculations reported here appear to support the simple model adopted in references [1, 2], indicating that refinements of the type outlined would introduce minor changes at the expense of much computational effort. A further consideration arguing against too elaborate modeling attempts is the inherent uncertainty as to the effects of surface impurity and roughness.

Acknowledgement

This work was supported in part by The National Science Foundation under Grant OIP75-01317 through the joint US-Polish Marie Sklodowska-Curie Research Fund and under Grant ENG75-22850. This support is gratefully acknowledged.

References

1. J. MIKIELEWICZ, J. R. MOSZYŃSKI, *Breakdown of a shear driven liquid film*, Transactions, Institute for Fluid Flow Machines, 66, p. 3, 1975.

http://rcin.org.pl

2. J. MIKIELEWICZ, J. R. MOSZYŃSKI, *Minimum thickness of a liquid film flowing vertically down a solid surface*, International Journal of Heat and Mass Transfer, **19**, p. 771, 1976.
3. S. G. BANKOFF, *Stability of a liquid flow down a heated inclined plane*, International Journal of Heat and Mass Transfer, **14**, p. 377, 1971.
4. T. HOBLER, *Minimal surface wetting* [in Polish], Chemia Stosowana, **2B**, p. 145, 1964.
5. T. HOBLER, J. CZAJKA, *Minimal wetting of a flat surface* [in Polish], Chemia Stosowana, **2B**, 169, 1968.
6. S. SEMICZEK-SZULC, J. MIKIELEWICZ, *The influence of surface roughness and the pressure of a gaseous medium on the wettability of metals*, 7th Symposium on Thermophysical Properties ASME/NBS, Gaithersburg, Md., May 1977, p. 864.
7. E. IHNATOWICZ, S. GUMKOWSKI, J. MIKIELEWICZ, *Experimental study of evaporation and breakdown of thin liquid films driven by shear stresses* [to be published in ASME J. of Heat Transfer].
8. D. WURZ, Doctoral Dissertation, Technical University of Karlsruhe 1975.
9. F. G. HAMMITT, *Flow of wet steam and related phenomena* [to be published].
10. V. A. THERNUHIN, *Experimental determination of the liquid film thickness and the entrainment flux* [in Russian], Izviestija Vyzshych Utchebnych Zaviedienij, Mashinostroenije, 4, p. 107, 1965.

POLISH ACADEMY OF SCIENCES,
INSTITUTE FOR FLUID FLOW MACHINES, GDAŃSK, POLAND
and
UNIVERSITY OF DELAWARE, NEWARK, DELAWARE, USA.

Received September 27, 1977.

http://rcin.org.pl